ChemComm

Cite this: *Chem. Commun.*, 2012, **48**, 6520–6522

www.rsc.org/chemcomm

COMMUNICATION

Electron-poor *N*-substituted imide-fused corannulenes†

Bernd M. Schmidt, Berit Topolinski, Philipp Roesch and Dieter Lentz*

Received 13th April 2012, Accepted 4th May 2012
DOI: 10.1039/c2cc32643d

***N*-Substituted imide-fused corannulenes can be generated from the corresponding tetramethylfluoranthenes. Syntheses, crystal structure and electronic properties are reported. The solid state structure of the pentafluorophenyl derivative shows nearly perfect π-stacking in a convex–concave fashion and is expected to possess useful electronic properties.**

Intensive attention has been paid to the development of organic semiconducting materials for the fabrication of devices such as organic thin-film transistors (OTFTs), organic photovoltaic cells (OPVs) as well as light-emitting diodes. Oligothiophenes,[1] fullerenes,[2] porphyrins[3] and especially (core-substituted) perylene ((C)PBI) and naphthalene bisimide ((C)NBI) dyes gained much popularity during the last few years.[4] In particular electron deficient PBIs are discussed as promising air-stable organic n-type semiconductors in thin film transistors. Curved polycyclic aromatic hydrocarbons are less studied, Seki and co-workers investigated the anisotropic electron-transport properties of the needle-like crystals of sumanene in 2009 and showed that high electron mobility can be examined by time-resolved microwave conductivity methods.[5] Both sumanene ($C_{21}H_{21}$)[6] and the shallower congener corannulene ($C_{20}H_{10}$) are non-planar subunits (buckybowls) of fullerenes. The latter buckybowl has been the subject of extensive theoretical and experimental research[7] and is now available in the kilogram scale.[8]

Recently, we investigated some intrinsic molecular properties of sumanene and corannulene, in particular their charge density distribution.[9] The crystal structure of sumanene is characterized by 1D columnar π-stacking in a convex–concave fashion,[10] whereas the solid state structure of unsubstituted corannulene is dominated by C–H$\cdots\pi$ interactions.[11] Nevertheless, depending on the substituent attached, different architectures can be formed in the solid state and have been investigated crystallographically. Siegel and co-workers showed for example that tetrabromocorannulene and di-, tetra- and pentasubstituted aryl-alkynylcorannulenes form columnar structures in the solid state.[12] Furthermore metal–organic assemblies like the binary complex of corannulene and a trimercury complex[13] as well as a Cu(111)[14] surface have been used to change the intermolecular alignment. The group of Petrukhina showed that the "hub" of corannulene can be reacted with electrophiles, leading to bowl-shaped carbocations bearing the counteranion partially.[15]

Corannulene-bowl based systems offer notionally a large π–π overlap if aligned in a convex–concave stacked fashion, comparable to or surpassing the overlapping surface of PBIs. A dense arrangement in the solid state could prevent the intrusion of oxygen and moisture into the channel region and might be important in the design of air-stable n-channel type semiconductors.

Herein we report the synthesis of corannulene-fused imides, a comparison with the fluoranthene precursor molecules as well as the isolation of by-products (Scheme 1). Solvent-free single-crystals of **1a**, **2** and **3a** could be obtained and the packing motifs were studied by X-ray crystal structure analysis.‡

N-Substituted maleimides can be easily prepared bearing various substituents.[16] Because of the very low nucleophilicity of (per)fluorinated amines, a late introduction is unfavorable. In combination with the method published by Siegel and co-workers[17] as well as other groups,[18] the corresponding fluoranthenes can

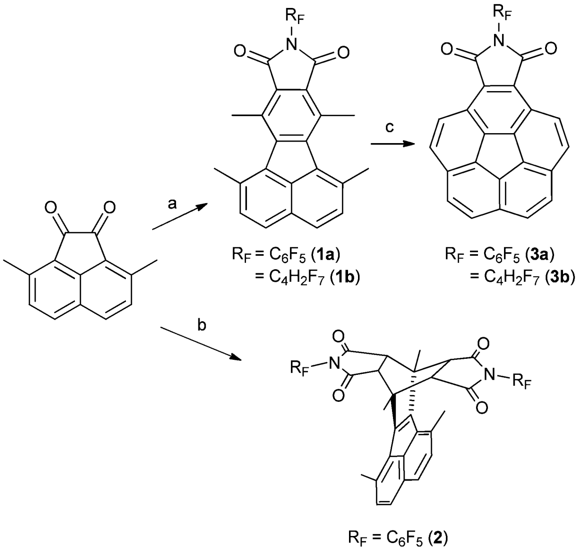

Scheme 1 (a) 4.8 eq. pentan-3-one, 7.5 eq. KOH, MeOH, 1 h rt; then 1.0 eq. of the corresponding maleimide, nitrobenzene, 48 h 180 °C; (b) 4.8 eq. pentan-3-one, 7.5 eq. KOH, MeOH, 1 h rt; then 1.0 eq. 1-(perfluorophenyl)-1H-pyrrole-2,5-dione, acetic anhydride, 48 h 140 °C; (c) 12.0 eq. NBS, 3.0 mol% DBPO, CCl_4, *hν*, 30 h 80 °C; then 8.8 eq. nickel powder, DMF, 8 h, 80 °C.

Freie Universität Berlin, Fabeckstrasse 34/36, D-14195, Berlin, Germany. E-mail: dlentz@zedat.fu-berlin.de; Fax: +49-30-838-52590; Tel: +49-30-838-52695

† Electronic supplementary information (ESI) available: Syntheses, X-ray crystallographic details and additional data. CCDC 876633–876635. For ESI and crystallographic data in CIF or other electronic format see DOI: 10.1039/c2cc32643d

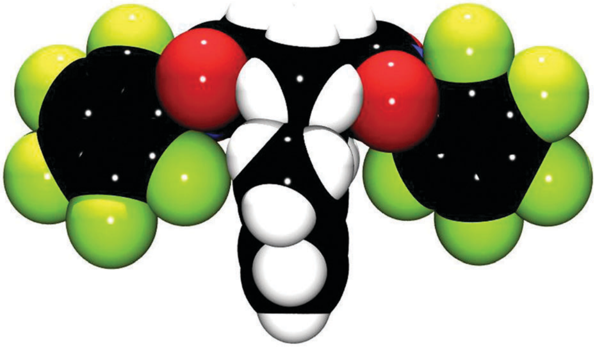

Fig. 1 Space-filling model of **2** as represented by the asymmetric unit, created with ORTEP[21] and rendered with POV-Ray.[22]

be prepared from 3,8-dimethylacenaphthene-quinone.[7b] The fluoranthene skeleton is thus constructed by condensation with pentan-3-one and subsequent Diels–Alder-reaction with the corresponding maleimides followed by decarbonylation. In this particular case however, the usage of acetic anhydride enables the formation of the adduct **2** with a central bicyclo[2.2.2]oct-2-ene unit, which is obtained as the major product. It is formed either by reaction of an exo-dimer from the condensation reaction or by decarbonylation of the exo-adduct and subsequent reaction with a second equivalent of maleimide.[19] Due to the molecular strain and steric repulsion,[20] the pentafluorophenyl group gives a distinct set of signals identifiable as the first order ABCDE-type ^{19}F-NMR spectrum at room temperature (see ESI†). The structure was ultimately assigned by single-crystal X-ray diffraction and is shown in Fig. 1.

If the reaction is run in nitrobenzene at 180 °C this adduct is not observed and the desired product **1a** and **1b** can be isolated in 43% and 45% yield, respectively. The steric hindrance in **2** and **1a** is expected to be similar, but now a fast C_6F_5 rotation is present in **1a** at room temperature, whereas no unusual characteristics are found for **1b**. The higher symmetry of **1a** in comparison to **2** now results in a AA′BB′C-type ^{19}F-NMR spectrum. The solid state structure shows a moderately canted alignment of the perfluorinated phenyl group in **1a**, which opposes the electron rich lower part ("naphthalene-part") of an adjacent molecule in the twisted stack, see Fig. 2. This dense head-to-tail crystal packing is supported by C–H···O bonding of the carbonyl groups of approximately 2.48 Å to the opposing molecule and furthermore by relevant C–F···H–C contacts[23] of 2.55 Å to the naphthalene-part of the next column (see ESI† for additional representations).

Wohl–Ziegler reaction and subsequent nickel-mediated intramolecular coupling involving complete debromination of the product[24] yield the corresponding corannulenes **3a** and **3b**, likewise. Single crystals of sufficient quality were obtained by slow evaporation of a chloroform solution. The bowls of **3a** are aligned into 1D parallel columns (see Fig. 3), but unlike for example indenocorannulenes,[25] in a staggered conformation.

The bowl direction of the same stack is the same, whereas adjacent columns have an opposite direction. The extended π-system results surprisingly in a shallower bowl-depth of about 0.826 Å, with the bowls being slightly tilted by 10°. This alignment is facilitated by C–H···F–C (2.55–2.78 Å) interactions between the anti-parallelly aligned neighboring stacks. The pentafluorophenyl ring is more canted in comparison to **1a**, with an angle of 76° to the imide ring, probably to maximize C–F···H–C contacts, and lacks the very close and flexible π-electron rich surface of **1a**. The ^{19}F-NMR spectrum at room temperature suggests again free rotation of the pentafluorophenyl ring of **3a** and the alkyl chain of **3b**. One spoke bond and one flank bond are the shortest (C_{016}–C_{031}) and longest (C_{019}–C_{034}) C–C-bonds of 1.3761(1) and 1.4453(1) Å in the corannulene-bowl, respectively. Both are marginally longer than in the parent corannulene molecule[11b] as a consequence of the decreased curvature and similar to the ones of published PBIs.[4e] Within the convex–concave stacks no pitch or roll angle is found, resulting in no transverse shifting. The intermolecular bowl distance calculated between three molecules along the stack is 7.34 Å, which leads to an average bowl-to-bowl distance of 3.67 Å, regardless of the small slipping angle. This difference is smaller than previously reported for tetra- and penta-substituted corannulenes, which may result from the steric demand of the arylalkynyl groups attached.[12a]

Cyclic voltammetry on a DCM solution reveals only moderate lowering of the LUMO levels of the fluoranthenes,[26] probably

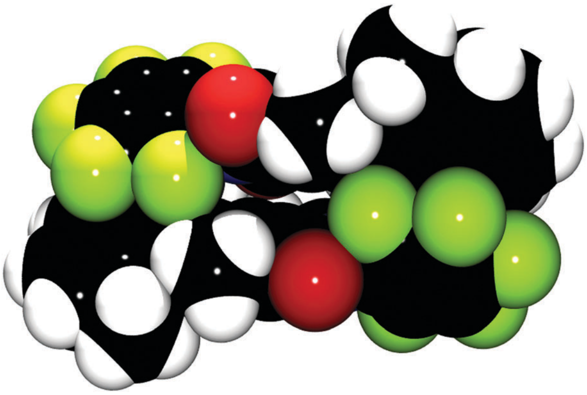

Fig. 2 ORTEP[21] representation (space-filling model) of the crystal packing in **1a**, rendered with POV-Ray.[22] The excerpt shows the dense head-to-tail arrangement which proceeds in infinite columns along the crystallographic *b* axis.

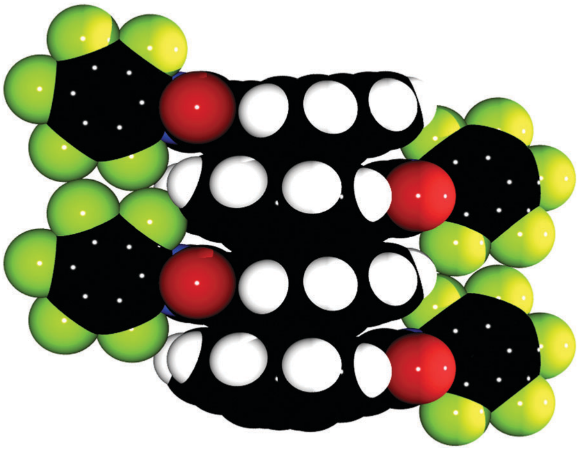

Fig. 3 Space-filling model of the crystal packing in **3a**, rendered with POV-Ray. The concave–convex bowl-in-bowl stacking is apparent, while the molecule's orientation and side chains alternate by roughly 180°.

because of the electron-donating methyl groups attached for the following ring-closure. The imide-fused corannulenes, **3a** and **3b**, show satisfactory LUMO energies of 3.4 eV for both compounds, especially when considering that only one section of the molecule is functionalized and no further bay substituents are present. The LUMO barrier is comparable to the one of unsubstituted PBI (3.8 eV)[27] and could be significantly lowered upon introduction of electron-withdrawing cyano substituents into the corannulene rim. The first reduction wave in dichloromethane solution to the monoanion is expected to take place at the extended node of the molecules. Measurements in THF show a well separated second reversible reduction wave to the dianion.

Imide-fused corannulenes can be generated easily by using cheap nickel powder, with aromatic or aliphatic imide substituents at the node of the conjugated system. The new class of corannulene compounds is promising for n-type semiconductor applications, because of their non-covalent interactions in the solid state. The twisted alignment of the bowls by nearly 180° provides additional shielding by the separated side chain. The large π–π overlap from the convex–concave stacked structure is highly favourable for charge carrier mobility. We will further investigate the optical and solid state properties of this new scaffold in due course.

Support from the Graduate School GRK 1582 is gratefully acknowledged. We thank Dr Holger Ott, Bruker-AXS, for the data collection of compound **3a** and Dr Shuhei Higashibayashi for valuable discussion.

Notes and references

‡ Crystal data for **1a**: $C_{28}H_{16}F_5NO_2$, monoclinic, a = 16.691(5) Å, b = 7.731(2) Å, c = 16.655(5) Å, α = 90.00°, β = 107.022(6)°, γ = 90.00°, V = 2055.0(11) Å^3, T = 133(2) K, space group $P2(1)/c$, Z = 4, 15 784 reflections measured, 3602 independent reflections (R_{int} = 0.0566). The final R_1 value was 0.0409 ($I > 2\sigma(I)$). The final w$R(F^2)$ value was 0.1078 ($I > 2\sigma(I)$). The final R_1 value was 0.0725 (all data). The final w$R(F^2)$ value was 0.1324 (all data). The goodness of fit on F^2 was 1.038. Crystal data for **2**: $C_{38}H_{20}F_{10}N_2O_4$, monoclinic, a = 12.407(4) Å, b = 27.476(8) Å, c = 9.607(3) Å, α = 90.00°, β = 110.687(6)°, γ = 90.00°, V = 3063.9(15) Å^3, T = 133(2) K, space group Cc, Z = 4, 17 831 reflections measured, 3125 independent reflections (R_{int} = 0.0565). The final R_1 value was 0.0463 ($I > 2\sigma(I)$). The final w$R(F^2)$ value was 0.1139 ($I > 2\sigma(I)$). The final R_1 value was 0.0648 (all data). The final w$R(F^2)$ value was 0.1235 (all data). The goodness of fit on F^2 was 1.061. Crystal data for **3a**: $C_{28}H_8F_5NO_2$, monoclinic, a = 16.4353(5) Å, b = 7.3459(2) Å, c = 16.4520(4) Å, α = 90.00°, β = 108.036(2)°, γ = 90.00°, V = 1888.68(9) Å^3, T = 100(2) K, space group $P2_1/n$, Z = 4, 17 814 reflections measured, 3883 independent reflections (R_{int} = 0.0530). The final R_1 value was 0.0373 ($I > 2\sigma(I)$). The final w$R(F^2)$ value was 0.0883 ($I > 2\sigma(I)$). The final R_1 value was 0.0535 (all data). The final w$R(F^2)$ value was 0.0961 (all data). The goodness of fit on F^2 was 1.019.

1 S. Allard, M. Forster, B. Souharce, H. Thiem and U. Scherf, *Angew. Chem., Int. Ed.*, 2008, **47**, 4070–4098.
2 P. M. Beaujuge and J. M. J. Fréchet, *J. Am. Chem. Soc.*, 2011, **133**, 20009–20029.
3 C.-C. You, R. Dobrawa, C. Saha-Möller and F. Würthner, Springer, Berlin/Heidelberg, 2005, vol. 258, pp. 39–82.
4 (*a*) L. Flamigni, B. Ventura, C.-C. You, C. Hippius and F. Würthner, *J. Phys. Chem. C*, 2006, **111**, 622–630; (*b*) M. Gsänger, J. H. Oh, M. Könemann, H. W. Höffken, A.-M. Krause, Z. Bao and F. Würthner, *Angew. Chem., Int. Ed.*, 2010, **49**, 740–743; (*c*) C. Huang, S. Barlow and S. R. Marder, *J. Org. Chem.*, 2011, **76**, 2386–2407; (*d*) R. Schmidt, M. M. Ling, J. H. Oh, M. Winkler, M. Könemann, Z. Bao and F. Würthner, *Adv. Mater.*, 2007, **19**, 3692–3695; (*e*) R. d. Schmidt, J. H. Oh, Y.-S. Sun, M. Deppisch, A.-M. Krause, K. Radacki, H. Braunschweig, M. Könemann, P. Erk, Z. Bao and F. Würthner, *J. Am. Chem. Soc.*, 2009, **131**, 6215–6228; (*f*) F. Würthner, C. Thalacker, S. Diele and C. Tschierske, *Chem.–Eur. J.*, 2001, **7**, 2245–2253.
5 T. Amaya, S. Seki, T. Moriuchi, K. Nakamoto, T. Nakata, H. Sakane, A. Saeki, S. Tagawa and T. Hirao, *J. Am. Chem. Soc.*, 2008, **131**, 408–409.
6 (*a*) H. Sakurai, T. Daiko and T. Hirao, *Science*, 2003, **301**, 1878; (*b*) T. Amaya and T. Hirao, *Chem. Commun.*, 2011, **47**, 10524–10535; (*c*) S. Higashibayashi and H. Sakurai, *Chem. Lett.*, 2011, 122–128.
7 (*a*) V. M. Tsefrikas and L. T. Scott, *Chem. Rev.*, 2006, **106**, 4868–4884; (*b*) Y.-T. Wu and J. S. Siegel, *Chem. Rev.*, 2006, **106**, 4843–4867; (*c*) A. Sygula, *Eur. J. Org. Chem.*, 2011, 1611–1625.
8 A. M. Butterfield, B. Gilomen and J. S. Siegel, *Org. Process Res. Dev.*, 2012, **16**, 664–676.
9 (*a*) S. Grabowsky, M. Weber, Y.-S. Chen, D. Lentz, B. M. Schmidt, M. Hesse and P. Luger, *Z. Naturforsch., B: Chem. Sci.*, 2010, **65**, 452–460; (*b*) S. Mebs, M. Weber, P. Luger, B. M. Schmidt, H. Sakurai, S. Higashibayashi, S. Onogi and D. Lentz, *Org. Biomol. Chem.*, 2012, **10**, 2218–2222.
10 H. Sakurai, T. Daiko, H. Sakane, T. Amaya and T. Hirao, *J. Am. Chem. Soc.*, 2005, **127**, 11580–11581.
11 (*a*) J. C. Hanson and C. E. Nordman, *Acta Crystallogr., Sect. B*, 1976, **32**, 1147–1153; (*b*) M. A. Petrukhina, K. W. Andreini, J. Mack and L. T. Scott, *J. Org. Chem.*, 2005, **70**, 5713–5716.
12 (*a*) Y.-T. Wu, D. Bandera, R. Maag, A. Linden, K. K. Baldridge and J. S. Siegel, *J. Am. Chem. Soc.*, 2008, **130**, 10729–10739; (*b*) L. Zoppi, L. Martin-Samos and K. K. Baldridge, *J. Am. Chem. Soc.*, 2011, **133**, 14002–14009.
13 (*a*) A. S. Filatov, A. K. Greene, E. A. Jackson, L. T. Scott and M. A. Petrukhina, *J. Organomet. Chem.*, 2011, **696**, 2877–2881; (*b*) A. S. Filatov, E. A. Jackson, L. T. Scott and M. A. Petrukhina, *Angew. Chem., Int. Ed.*, 2009, **48**, 8473–8476.
14 T. Bauert, K. K. Baldridge, J. S. Siegel and K.-H. Ernst, *Chem. Commun.*, 2011, **47**, 7995–7997.
15 (*a*) A. V. Zabula, C. Dubceac, A. S. Filatov and M. A. Petrukhina, *J. Org. Chem.*, 2011, **76**, 9572–9576; (*b*) A. V. Zabula, S. N. Spisak, A. S. Filatov, A. Y. Rogachev and M. A. Petrukhina, *Angew. Chem., Int. Ed.*, 2011, **50**, 2971–2974.
16 A. Schwarzer and E. Weber, *Cryst. Growth Des.*, 2008, **8**, 2862–2874.
17 (*a*) A. Borchardt, A. Fuchicello, K. V. Kilway, K. K. Baldridge and J. S. Siegel, *J. Am. Chem. Soc.*, 1992, **114**, 1921–1923; (*b*) T. J. Seiders, E. L. Elliott, G. H. Grube and J. S. Siegel, *J. Am. Chem. Soc.*, 1999, **121**, 7804–7813.
18 (*a*) A. Sygula and P. W. Rabideau, *J. Am. Chem. Soc.*, 1998, **120**, 12666–12667; (*b*) A. Sygula and P. W. Rabideau, *J. Am. Chem. Soc.*, 1999, **121**, 7800–7803; (*c*) A. Sygula and P. W. Rabideau, *J. Am. Chem. Soc.*, 2000, **122**, 6323–6324.
19 (*a*) D. W. Jones and W. S. McDonald, *J. Chem. Soc., Chem. Commun.*, 1980, 417–418; (*b*) M. Krivec, M. Gazvoda, K. Kranjc, S. Polanc and M. Kočevar, *J. Org. Chem.*, 2012, **77**, 2857–2864.
20 K. Bynum, R. Prip, R. Callahan and R. Rothchild, *J. Fluorine Chem.*, 1998, **90**, 39–46.
21 L. Farrugia, *J. Appl. Crystallogr.*, 1997, **30**, 565.
22 Persistence of Vision Pty. Ltd. http://www.povray.org/.
23 R. Berger, G. Resnati, P. Metrangolo, E. Weber and J. Hulliger, *Chem. Soc. Rev.*, 2011, **40**, 3496–3508.
24 A. Sygula, S. D. Karlen, R. Sygula and P. W. Rabideau, *Org. Lett.*, 2002, **4**, 3135–3137.
25 A. S. Filatov, L. T. Scott and M. A. Petrukhina, *Cryst. Growth Des.*, 2010, **10**, 4607–4621.
26 L. Ding, H.-Z. Ying, Y. Zhou, T. Lei and J. Pei, *Org. Lett.*, 2010, **12**, 5522–5525.
27 A. Pron, P. Gawrys, M. Zagorska, D. Djurado and R. Demadrille, *Chem. Soc. Rev.*, 2010, **39**, 2577–2632.